

## From strong interactions to Dark Matter: the non-perturbative QCD sphaleron rate

---

**Claudio Bonanno**<sup>a,b,\*</sup>

<sup>a</sup>*Instituto de Física Teórica UAM-CSIC, Calle Nicolás Cabrera 13-15,  
Universidad Autónoma de Madrid, Cantoblanco, E-28049 Madrid, Spain*

<sup>b</sup>*Albert Einstein Center for Fundamental Physics, Institute for Theoretical Physics, University of Bern,  
Sidlerstraße 5, CH-3012 Bern, Switzerland*

*E-mail:* [claudio.bonanno@unibe.ch](mailto:claudio.bonanno@unibe.ch)

Acceptance plenary talk for the 2025 Kenneth G. Wilson Award for Excellence in Lattice Field Theory: *For significant contributions to the understanding of topology in QCD, QCD-like, and large- $N_c$  gauge theories, including algorithmic developments to reduce topological freezing, studies of Dirac spectral properties, and axion phenomenology.*

*The 42<sup>nd</sup> International Symposium on Lattice Field Theory (LATTICE2025)  
2–8 November 2025  
Tata Institute of Fundamental Research, Mumbai, India*

---

\*Speaker

## **Kenneth G. Wilson Award**

Having been selected as the recipient of the 2025 Kenneth G. Wilson Award (KWA) for Excellence in Lattice Field Theory is an immense honor. When I received the news, I could not help but thinking about how exciting it is to be part of the large and diverse community working on Lattice Field Theory, initiated by Wilson’s fundamental work on confinement. What I find particularly stimulating is that, being Lattice Field Theory sitting at the crossroad between Physics, Mathematics and Computational Sciences, many different expertise had to come together to make progress in this field possible. In my professional experience so far, I have done my best to give my own contributions to these three facets of Lattice Field Theory — theory, phenomenology, and algorithms. I am extremely grateful to the KWA Selection Committee, to the International Advisory Committee, and to the Lattice 2025 conference organizers, for acknowledging my contributions. I am also extremely grateful for all the warm and sincere expressions of esteem I have received after this recognition from many other colleagues.

Clearly, I would have never reached this achievement without the invaluable role of my collaborators, and without the excellent work environment provided by Pisa, Arcetri, Firenze, Madrid, and now Bern. I have been blessed with the possibility of being part of fruitful scientific environments that fostered my professional development, and of collaborating with many excellent scientists. I would like to extend my heartfelt thanks to all my collaborators and to all the colleagues I have scientifically interacted with for making research such a stimulating and positive experience. I will not list all of you, but I must make two exceptions. First, I want to thank Massimo D’Elia for having been the best professor, supervisor, mentor, and collaborator, over the almost-decade we have been working together. Your sincere encouragement and support helped me to find my own way in research. In the years to come, I aspire to follow the model of mentorship and supervision you represent. Then, I want to thank Margarita García Pérez for making my three years in Madrid one of the most formative experiences of my life. The countless discussions about physics, and beyond, with you made me grow both as a person and as a researcher. You have taught me so many things — including Spanish, by talking to me in your beautiful language — and I would like to express my gratitude to you for being such a wonderful person and collaborator. ¡Muchas gracias!

In what follows, I will propose a transcript of the KWA acceptance plenary talk I have given at Lattice 2025. In that contribution, I decided to present the main findings of the papers [1–3] for three main reasons. First, they constitute my and my collaborators’ latest contributions to the topics mentioned in the award. Secondly, I believe they can be of broad interest both to the Lattice community and to scientists working in neighboring fields. Finally, they allow me to delineate what are possible future directions to further develop the field of investigation cited in the award.

### **1. Theoretical and phenomenological implications of the strong sphaleron rate**

Since the pioneering works of Witten [4] and Veneziano [5], it has been clear that gauge topology plays a prominent role in determining many of the salient theoretical features of gauge theories, with fundamental implications for phenomenology. Topological properties of gauge theories stem from purely non-perturbative dynamics, and Lattice Quantum Chromo-Dynamics (QCD) has been instrumental to address this topic from first principles. By now, there are several topics in gauge

topology that have been extensively addressed from the lattice, such as  $\theta$ -dependence and its connection with the Witten–Veneziano mechanism [6–14] and with axion phenomenology [15–24], the neutron electric dipole moment [25–31], the role of topology in the QCD phase diagram [32–36], and more. This article is about a topic in gauge topology that has received far less attention from the lattice: *real-time sphaleron transitions* in strong interactions.

Sphalerons are unstable field configurations corresponding to saddle-points of the Yang–Mills action in Minkowski time [37–39]. At the semiclassical level, they can be interpreted as describing transitions among topologically-non-equivalent vacua due to thermal fluctuations above potential barriers separating them, see the cartoon in Fig. 1. Thus, unlike the *suppressed* quantum tunneling through the barrier via instantons [40], sphalerons are *enhanced* at high temperatures [37, 38]. The name “sphaleron” was exactly coined to capture these features [38], as it comes from the Greek word σφᾶλερός (sphālerós), which can be translated as “slippery, ready to fall”.

An intriguing physical observable related to sphaleron configurations is the strong *sphaleron rate*  $\Gamma_s$ , the rate of real-time (i.e., Minkowski time) sphaleron transitions in QCD. It is defined as:

$$\Gamma_s \equiv \int d^3x dt \langle q(\vec{x}, t) q(\vec{0}, 0) \rangle_T. \quad (1)$$

Here,  $q(\vec{x}, t)$  is the topological charge density:

$$q(\vec{x}, t) = \frac{1}{16\pi^2} \text{Tr} \left[ G_{\mu\nu}(\vec{x}, t) \tilde{G}^{\mu\nu}(\vec{x}, t) \right], \quad (2)$$

with  $G_{\mu\nu} = \partial_\mu A_\nu - \partial_\nu A_\mu + i[A_\mu, A_\nu]$  and  $\tilde{G}_{\mu\nu} = \frac{1}{2}\epsilon_{\mu\nu\rho\sigma} G^{\rho\sigma}$  the gauge field strength and its dual tensor. The thermal expectation value  $\langle \dots \rangle_T$  in Eq. (1) is defined as:

$$\langle q(\vec{x}, t) q(\vec{0}, 0) \rangle_T \equiv \frac{1}{Z(T)} \text{Tr} \left\{ e^{-\mathcal{H}_{\text{QCD}}/T} q(\vec{x}, t) q(\vec{0}, 0) \right\}, \quad Z(T) \equiv \text{Tr} \left\{ e^{-\mathcal{H}_{\text{QCD}}/T} \right\}. \quad (3)$$

From the discussion so far, it is clear that the QCD sphaleron rate is a physical quantity characterizing the intricate non-perturbative dynamics of strong interactions, and has thus deep theoretical significance *per se*. In addition to this, however, it is also of great phenomenological relevance, both for collider physics and for Dark Matter searches.

Concerning collider physics, by virtue of the axial anomaly [41], sphaleron transitions can create chiral imbalances [37], i.e., an excess of left-handed or right-handed fermion excitations:  $N_R - N_L \neq 0$ . If such an event takes place in a hot, dense and magnetized out-of-equilibrium strongly-interacting medium, such as the fireball forming for few instants after a heavy-ion collision (see, e.g., Ref. [42]), this can lead to a phenomenon known as the *Chiral Magnetic Effect* (CME) [43–46].

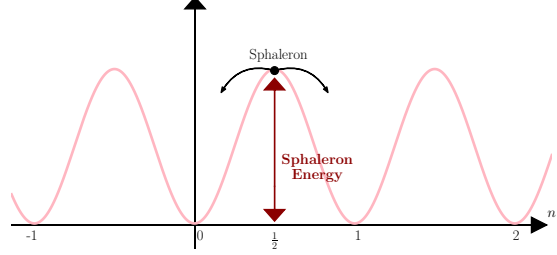


**Figure 1:** Semiclassical cartoon of the landscape of topologically-non-equivalent Yang–Mills vacua, labeled by an integer winding number  $n$ , and of a sphaleron transition above the potential barrier.

In a few words, the coupling between the quark electric charges and the external magnetic field causes an alignment of quark spins along the magnetic field itself. When quark excitations carry also a definite chirality, this in turns causes also an alignment of their momenta along the magnetic field direction. Therefore, the presence of an imbalance between left-handed and right-handed modes, caused by a sphaleron transition, leads to a net electric current flowing in the medium in the parallel direction to the magnetic field. This is illustrated in the cartoon in Fig. 2. In this context, the sphaleron rate describes the relaxation of the axial quark number density  $\rho_5$  as the medium equilibrates in the presence of  $N_f^{(\ell)}$  light quark species [47, 48]:

$$\frac{d\rho_5}{dt} = -\frac{N_f^{(\ell)}}{T^3} \Gamma_s \rho_5. \quad (4)$$

Signatures of the CME are currently being searched in heavy-ion collision experiments, see, e.g., Ref. [49], thus theoretical inputs about  $\Gamma_s$  are of the utmost importance for this quest.

In the context of Dark Matter cosmological searches, instead, the QCD sphaleron rate  $\Gamma_s$ , and its generalization to non-zero momenta (sometimes simply called the ‘‘topological rate’’):

$$\Gamma(E, p) = \int d^3x dt e^{ip^\mu x_\mu} \langle q(\vec{x}, t) q(\vec{0}, 0) \rangle_T, \quad \Gamma_s = \Gamma(0, 0), \quad p^\mu = (E, \vec{p}), \quad p = |\vec{p}|, \quad (5)$$

play instead a very important phenomenological role for QCD axion physics [50–53]. In the hot cosmological medium permeating the early Universe, sphaleron transitions are effective in creating hot axions by virtue of the axion-gluon interaction term  $\propto a(x)q(x)$ . This process is expected to have happened out of equilibrium, thus, in order to compute the time-evolution of the axion number distribution function  $f_p$ , one has to solve the following Boltzmann equation [50],

$$\frac{df_p}{dt} = (1 + f_p) \Gamma_p^{(+)} - f_p \Gamma_p^{(-)}, \quad (6)$$

where the axion creation/annihilation rates  $\Gamma_p^{(+)} / \Gamma_p^{(-)}$  are given by:

$$\Gamma_p^{(-)} = e^{\frac{E(p)}{T}} \Gamma_p^{(+)} = \frac{1}{2E(p)f_a} \Gamma(E(p), p), \quad E^2(p) = m_a^2 + p^2, \quad (7)$$

with  $m_a$  and  $f_a$  the axion mass and decay constant respectively. Theoretical estimates to compute the abundance of relic axions, which can in principle be measured by upcoming cosmological surveys, require the non-perturbative QCD topological rate as a fundamental input, especially for temperatures around and above the QCD chiral crossover, where non-perturbative effects are important.

Due to its theoretical and phenomenological importance, and by virtue of its intrinsic non-perturbative nature (especially at the temperatures of interest for physical applications), Lattice

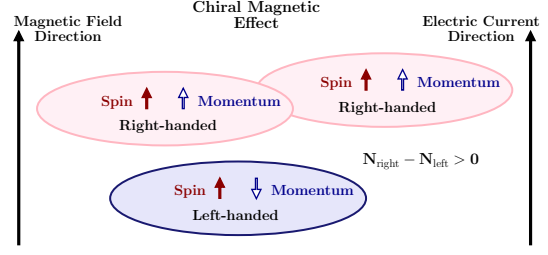


**Figure 2:** Cartoon representing the Chiral Magnetic Effect in the presence of a sphaleron-induced quark chiral imbalance.

QCD seems a natural tool to compute the QCD sphaleron rate from first principles. However, being Monte Carlo calculations of lattice-regularized Quantum Field Theory based on the Euclidean formulation, this is an highly non-trivial task due to the inherent real-time nature of the sphaleron rate. More precisely, using analytic continuation, one can only relate the sphaleron rate to an Euclidean correlation function via a convolutional integral relation. Let us introduce the Euclidean time correlator of the topological charge density:

$$G_E(\tau) = \int d^3x \langle q(\vec{x}, \tau) q(\vec{0}, 0) \rangle, \quad \int d^4x q(x) = Q \in \mathbb{Z}, \quad (8)$$

with  $Q$  the integer-valued topological charge,  $\tau$  the Euclidean time separation, and where  $\langle \dots \rangle$  stands for the Euclidean path integral expectation value computed in the presence of a compactified temporal direction with length  $1/T$ . Introducing the thermal spectral density  $\rho(\omega)$  of  $G_E(\tau)$ ,

$$G_E(\tau) = - \int_0^\infty \frac{d\omega}{\pi} \rho(\omega) \frac{\cosh \left[ \omega \left( \tau - \frac{1}{2T} \right) \right]}{\sinh \left( \frac{\omega}{2T} \right)} \equiv - \int_0^\infty \frac{d\omega}{\pi} \rho(\omega) K(\omega, \tau), \quad (9)$$

the following relation holds [54, 55]:

$$\Gamma_s = 2T \lim_{\omega \rightarrow 0} \frac{\rho(\omega)}{\omega}. \quad (10)$$

In practice, extracting the sphaleron rate from a lattice calculation requires the calculation of  $G_E(\tau)$ , and then the inversion of Eq. (9) to extract the spectral density [related to  $\Gamma_s$  via Eq. (10)]. This task falls under a broad class of mathematical problems known as *inverse problems*. Inverse problems are notoriously difficult to solve numerically since they are ill-posed, i.e., even a small fluctuation of the input data can cause a huge change in the output results. Given that lattice-computed correlation functions are affected by statistical uncertainties and are only known for a discrete set of temporal separations, statistical errors on the spectral density will blow up if no strategy is employed to improve the conditioning of the inverse problem. This explains why, until a few of years ago, only a few preliminary lattice attempts to compute  $\Gamma_s$ , all limited to the SU(3) pure-gauge theory, have been performed [48, 56, 57].

In our recent paper [2], we significantly advanced the state of the art, providing the first non-perturbative investigation of  $\Gamma_s$  in  $N_f = 2 + 1$  QCD with physical quark masses in the temperature range  $1.5 \lesssim T/T_c \lesssim 4$ , with  $T_c \simeq 155$  MeV the QCD chiral crossover temperature. This advancement was possible thanks to the novel methodology we introduced in Ref. [1]. In recent years, many studies addressed possible numerical procedures to solve inverse problems in Lattice Field Theory [58–64]. The method of Ref. [1] exploits one of these new proposals, the Hansen–Lupo–Tantalo (HLT) method [59] — based on a non-trivial modification of the Backus–Gilbert method [65] — which has been extensively employed in recent years [66–75].

This manuscript is organized as follows. The new method of Ref. [1] is presented in Sec. 2. The results of Ref. [2] about the temperature dependence of the QCD sphaleron rate are discussed in Sec. 3. Finally, in Sec. 4, I will draw my conclusions and discuss future outlooks, and how algorithmic improvements of Ref. [3] will be key to achieve them.

## 2. Non-perturbative strong sphaleron rate from Lattice QCD: a novel approach

This section summarizes the method of [1] to compute the sphaleron rate from Lattice QCD.

## 2.1 The inverse problem resolution

Let us rewrite the target inverse problem as:

$$G_L(\tau) = - \int_0^\infty \frac{d\omega}{\pi} \frac{\rho_L(\omega)}{\omega} K'(\omega, \tau), \quad K'(\omega, \tau) = \omega K(\omega, \tau), \quad (11)$$

where  $G_L(\tau)$  is the lattice topological charge density correlator (whose calculation will be described in the next section 2.2), and  $\rho_L(\omega)$  its spectral density. Let us look for a solution for the spectral density of the form:

$$\frac{\bar{\rho}_L(\bar{\omega})}{\bar{\omega}} = -\pi \sum_{\tau=0}^{1/T} g_\tau(\bar{\omega}) G_L(\tau), \quad (12)$$

with  $g_\tau(\bar{\omega})$  unknown coefficients to be determined, and where the sum runs over the discretized times  $\tau = an_t$ ,  $n_t = 0, 1, \dots, N_t$ , with  $a$  the lattice spacing and  $N_t = 1/(aT)$  the number of lattice temporal sites. This implies that the lattice sphaleron rate  $\Gamma_L$  is given by:

$$\frac{1}{2T} \Gamma_L = \left. \frac{\bar{\rho}_L(\bar{\omega})}{\bar{\omega}} \right|_{\bar{\omega}=0} = -\pi \sum_{\tau=0}^{1/T} g_\tau G_L(\tau), \quad (13)$$

where  $g_\tau$  is a short-hand for  $g_\tau(\bar{\omega} = 0)$ . Combining Eq. (12) and Eq. (11), one obtains the following consistency relation:

$$\frac{\bar{\rho}_L(\bar{\omega})}{\bar{\omega}} = \int_0^\infty d\omega \Delta(\omega, \bar{\omega}) \frac{\rho_L(\omega)}{\omega}. \quad (14)$$

This is a *smearing relation* between the actual spectral density  $\rho_L(\omega)/\omega$  and the solution  $\bar{\rho}_L(\bar{\omega})/\bar{\omega}$ . The smearing kernel  $\Delta(\omega, \bar{\omega})$ , also known as *resolution function*, is given by:

$$\Delta(\omega, \bar{\omega}) = \sum_{\tau=0}^{1/T} g_\tau(\bar{\omega}) K'(\omega, \tau). \quad (15)$$

Determining the sphaleron rate has thus been rephrased into the problem of determining the coefficients  $g_\tau$  in such a way that  $\Delta(\omega) \equiv \Delta(\omega, \bar{\omega} = 0)$  is sufficiently peaked around  $\bar{\omega} = 0$ , so that  $\bar{\rho}_L(\bar{\omega})/\bar{\omega}$  is a good approximation of  $\rho_L(\omega)/\omega$  around the origin.

The HLT method exactly allows to determine the  $g_\tau$  coefficients from the minimization of the following functional:

$$F_\lambda[g] = (1 - \lambda)A_2[g] + \lambda B[g], \quad (16)$$

with

$$A_\alpha[g] = \int_0^\infty d\omega |\Delta(\omega) - \delta_\sigma(\omega)|^2 e^{\alpha\omega}, \quad B[g] = \frac{1}{G_L^2(0)} \sum_{\tau_1, \tau_2} \text{Cov}_{\tau_1 \tau_2} g_{\tau_1} g_{\tau_2}. \quad (17)$$

The functional  $A_2[g]$  expresses the difference between the smearing kernel  $\Delta(\omega)$  and a given target smearing kernel  $\delta_\sigma(\omega)$ , which can be chosen with a certain degree of arbitrariness. In [1, 2], inspired by the functional form of  $K'(\omega, \tau)$ , we chose:

$$\delta_\sigma(\omega) = \left( \frac{2}{\pi\sigma} \right)^2 \frac{\omega}{\sinh\left(\frac{\omega}{2T}\right)}, \quad \text{which satisfies} \quad \lim_{\sigma \rightarrow 0} \delta_\sigma(\omega) = \delta(\omega). \quad (18)$$

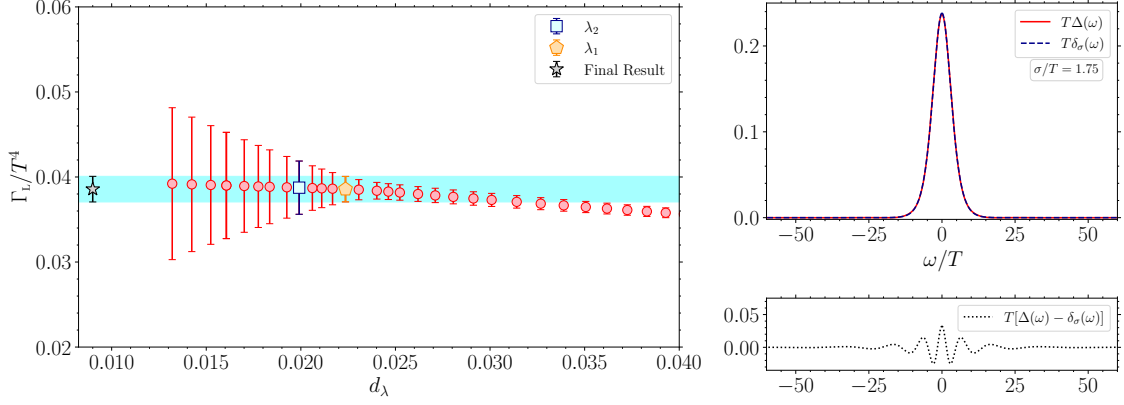


**Figure 3:** Left panel: example of the calculation of the sphaleron rate from the inverse problem resolution via the HLT method. Right panel: comparison between the reconstructed smearing kernel  $\Delta(\omega)$  for  $\lambda = \lambda_1$  and the chosen target one  $\delta_\sigma(\omega)$ . Figures from Ref. [1].

If the smearing kernel  $\Delta(\omega)$  is close enough to the target one  $\delta_\sigma(\omega)$ , its width around the desired point (the origin, in the case at hand) will be given by  $\sigma$ , which is an input of the HLT method. Being able to control  $\sigma$  is a great advantage of HLT over the original Backus–Gilbert, both because it allows to control possible systematic effects introduced by the smearing, and because it allows to keep it constant as other parameters (e.g., the lattice spacing) are varied. The functional  $B[g]$ , instead, is directly proportional to the statistical uncertainties on the lattice correlator  $G_L(\tau)$  via its covariance matrix  $\text{Cov}_{\tau_1\tau_2}$ , and acts as a regulator of the inverse problem.

The computation of the sphaleron rate requires to minimize  $F_\lambda[g]$  for several values of  $\lambda$  in order to look for the optimal trade-off between  $A_2[g]$  and  $B[g]$ , i.e., between statistical and systematic uncertainties. Indeed, when  $\lambda \rightarrow 0$  and  $A_2[g]$  dominates,  $\Delta(\omega)$  will be very close to  $\delta_\sigma(\omega)$ , but fluctuations on  $g_\tau$  will explode due to the inverse problem being ill-posed. As  $\lambda \rightarrow 1$ ,  $B[g]$  will dominate, and the inverse problem will be regularized. This will damp the fluctuations of  $g_\tau$  at the price of introducing a systematic error, due to the fact that the shape of  $\Delta(\omega)$  is unconstrained and the smearing procedure is out of control. The idea is therefore to vary  $\lambda$  and look for an intermediate regime where a plateau in the resulting values of  $\Gamma_L$  is observed. When such plateau is found before statistical errors explode, it signals that systematic errors are under control, and the plateau can be used to assess the final value and uncertainty of the sphaleron rate.

An example of this procedure is illustrated in the left panel of Fig. 3, while the right panel shows an example of the reconstructed smearing kernel versus the target one. Since  $\lambda$  typically varies across several orders of magnitude, it is better to look for a plateau in terms of the figure of merit:

$$d_\lambda = \sqrt{\frac{A_0[g_\tau^*(\lambda)]}{A_0[0]}}, \quad (19)$$

where  $g_\tau^*(\lambda)$  is the minimum of  $F_\lambda[g]$ . The quantity  $d_\lambda$  expresses the distance between the smearing kernel  $\Delta(\omega)$  and the target smearing kernel  $\delta_\sigma(\omega)$  for a given  $\lambda$ , and is thus a good figure of merit to quantify the reliability of the numerical solution of the inverse problem. Indeed, if  $d_\lambda$  is small, the reconstructed kernel is close to the target one, and one has control over the smearing of the spectral

density. Once a plateau for  $\Gamma_L$  as a function of  $d_\lambda$  is identified, we select two values  $\lambda_1 > \lambda_2$ . The value of the rate  $\Gamma_1$  corresponding to  $\lambda_1$  gives the central value and the statistical uncertainty of the final result. The value  $\Gamma_2$  corresponding to  $\lambda_2$  is used to assess the systematic error (which is summed in quadrature to the statistical one) via:

$$\text{Err}_{\text{sys}} = |\Gamma_1 - \Gamma_2| \text{erf} \left( \frac{1}{\sqrt{2}} \frac{|\Gamma_1 - \Gamma_2|}{\sqrt{\text{Err}_{\text{stat},1}^2 + \text{Err}_{\text{stat},2}^2}} \right). \quad (20)$$

## 2.2 Determination of the Euclidean topological charge density correlator

The determination of the Euclidean topological charge density correlator from the lattice is something that is challenging by itself. It is well known that gluonic lattice topological charge formulations, such as the customary lattice clover definition  $Q_{\text{clov}}$ ,

$$Q_{\text{clov}} = \sum_x q_{\text{clov}}(x) = \frac{1}{32\pi^2} \sum_x \sum_{\mu\nu\rho\sigma} \varepsilon_{\mu\nu\rho\sigma} \text{Tr} [C_{\mu\nu}(x)C_{\rho\sigma}(x)], \quad (21)$$

$$C_{\mu\nu}(x) = \frac{1}{4} \mathfrak{I} \{ U_{\mu\nu}(x) + U_{-\nu,\mu}(x) + U_{\nu,-\mu}(x) + U_{-\mu,-\nu}(x) \}, \quad (22)$$

$$U_{\mu\nu}(x) = U_\mu(x)U_\nu(x + a\hat{\mu})U_\mu^\dagger(x + a\hat{\nu})U_\nu^\dagger(x), \quad U_{-\mu}(x) = U_\mu^\dagger(x - a\hat{\mu}), \quad (23)$$

suffers for multiplicative renormalizations due to ultra-violet fluctuations at the scale of the lattice spacing. Moreover, further divergent additive renormalizations appear when computing integrals of correlation functions of  $q(x)$ , such as the topological susceptibility  $\chi = \langle Q^2 \rangle / V = \int d^4x \langle q(x)q(0) \rangle = \int d\tau G_E(\tau)$ . To deal with these renormalizations, it is customary to compute lattice gluonic topological charge definitions on smoothed gauge configurations. Thus, the lattice topological charge density correlator is computed on smoothed configurations too.

Smoothing introduces a new length scale in the game, the *smoothing radius*  $R_s$ , the scale below which fluctuations are damped. This scale is proportional to the square root of the amount of smoothing performed. Smoothing unavoidably modifies the short-distance behavior of the lattice correlator  $G_L(\tau)$ . This is clearly illustrated in Fig. 4. General theoretical arguments based on reflection positivity imply that the continuum correlator  $G_E(\tau)$  must be negative for every positive time separation  $\tau > 0$ . On the lattice, however, due to smoothing, this condition is violated when  $\tau < R_s$ . In this regime, the lattice correlator  $G_L(\tau)$  becomes positive and unphysical. The negativity of the correlator is only recovered in the limit  $R_s \rightarrow 0$ , which must be taken after the continuum limit  $a \rightarrow 0$ . This is shown in Fig. 4, which displays the negativity of the continuum correlator  $G_E(\tau)$ , obtained after the double extrapolation  $a \rightarrow 0$  and  $R_s \rightarrow 0$ .

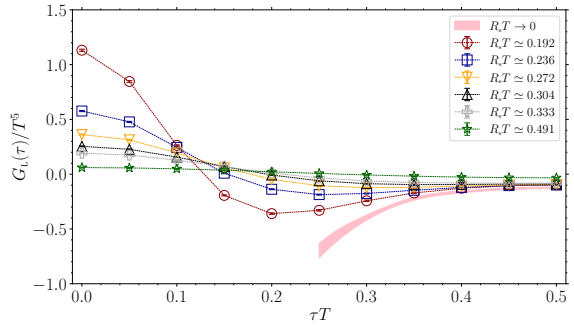


**Figure 4:** Comparison of determinations of  $G_L(\tau)$  at finite lattice spacing for a few values of  $R_s$  with the  $R_s \rightarrow 0$ -extrapolated continuum correlator  $G_E(\tau)$ . Figure from Ref. [1].

In our studies [1, 2] we employed cooling [76–80] as our smoothing method of choice. In this case, the square smoothing radius is proportional to the number of cooling steps:

$$\frac{R_s}{a} = \sqrt{\frac{8}{3}n_{\text{cool}}}. \quad (24)$$

Other smoothing methods, such as gradient flow [81–83] or stout smearing [84], have been shown to give consistent results once the smoothing radii are matched to one another [85] (see also [86]).

### 3. Numerical results for the QCD sphaleron rate

This section summarizes the main results of [2] about the QCD sphaleron rate.

#### 3.1 Controlling finite- $a$ , finite- $R_s$ , and finite- $\sigma$ effects on the sphaleron rate

Using the methods described in Sec. 2, in Ref. [2] we determined the sphaleron rate for 5 temperatures in the range  $1.5 \lesssim T/T_c \lesssim 4$  in full QCD with  $N_f = 2 + 1$  dynamical flavors, corresponding to a light quark doublet with mass  $m_\ell = m_u = m_d$  and a strange quark with mass  $m_s$ , both tuned at the physical point. More precisely, we tuned the bare parameters to have  $m_\pi = m_\pi^{(\text{phys})} \simeq 135$  MeV and  $R = m_\ell/m_s = R^{(\text{phys})} \simeq 0.036$ . Our simulations are performed at fixed spatial lattice size  $LT = 4$ , which is expected to be sufficiently large to avoid significant finite-volume effects. Due to the strong suppression of the topological susceptibility  $\chi \sim 1/T^8$  in the high-temperature phase of QCD, topological charge fluctuations become very rare since  $\langle Q^2 \rangle = \chi V = \chi L^3/T \sim 1/T^{12} \ll 1$ . This introduces a sampling problem in the topological charge, which in [2] we overcame by adopting a multicanonical algorithmic approach [20, 87, 88].

The sphaleron rate  $\Gamma_L$  is calculated for several lattice spacings  $aT = 1/N_t$ , for several values of the smoothing radius  $R_s T$  used to compute the lattice topological charge density correlator  $G_L(\tau)$ , and for several values of the smearing width  $\sigma/T$  used to solve the inverse problem via the HLT method. The final result was obtained in [2] as follows. First, we took the continuum limit  $aT \rightarrow 0$  at fixed  $R_s T$  and  $\sigma/T$ . Then, we took the limits  $R_s T \rightarrow 0$  and  $\sigma/T \rightarrow 0$  of the continuum results. In Fig. 5, the procedure to compute  $\Gamma_s$  is exemplified for  $T \simeq 300$  MeV, i.e.,  $T/T_c \simeq 1.94$ . The top left panel shows the Monte Carlo history of the topological charge. As it can be seen, our multicanonical simulations completely avoid the sampling problem of the topological charge due to the suppression of  $\langle Q^2 \rangle$  at high temperatures. The top right panel shows the continuum limit of  $\Gamma_L/T^4$  for the 3 smallest values of  $R_s T$  explored. All shown continuum limits are taken at fixed  $\sigma/T = 1.75$ . They all turn out to be rather smooth, and no significant difference is observed if the coarsest lattice spacing is included/excluded in the extrapolation. The bottom left panel shows the  $R_s$ -dependence of the continuum extrapolations of  $\Gamma_s/T^4$  for fixed  $\sigma/T = 1.75$ . As it can be seen, below  $R_s T \simeq 0.375$  the sphaleron rate exhibits a plateau as a function of the smoothing radius. The value of such plateau is taken as our  $R_s T \rightarrow 0$  limit. This behavior has a clear physical explanation: the smoothing radius  $R_s$  is a ultra-violet scale, while the sphaleron rate is the zero-frequency limit of the spectral density slope, which receives the dominant contributions from the large- $\tau$  tail (i.e.,  $\tau T$  close to 0.5) of the topological charge density correlator. Thus, when  $R_s$  is sufficiently small, there is an effective separation between these two scales, and  $\Gamma_s$  becomes independent of the smoothing radius. This is similar to what happens to the topological susceptibility, which also becomes

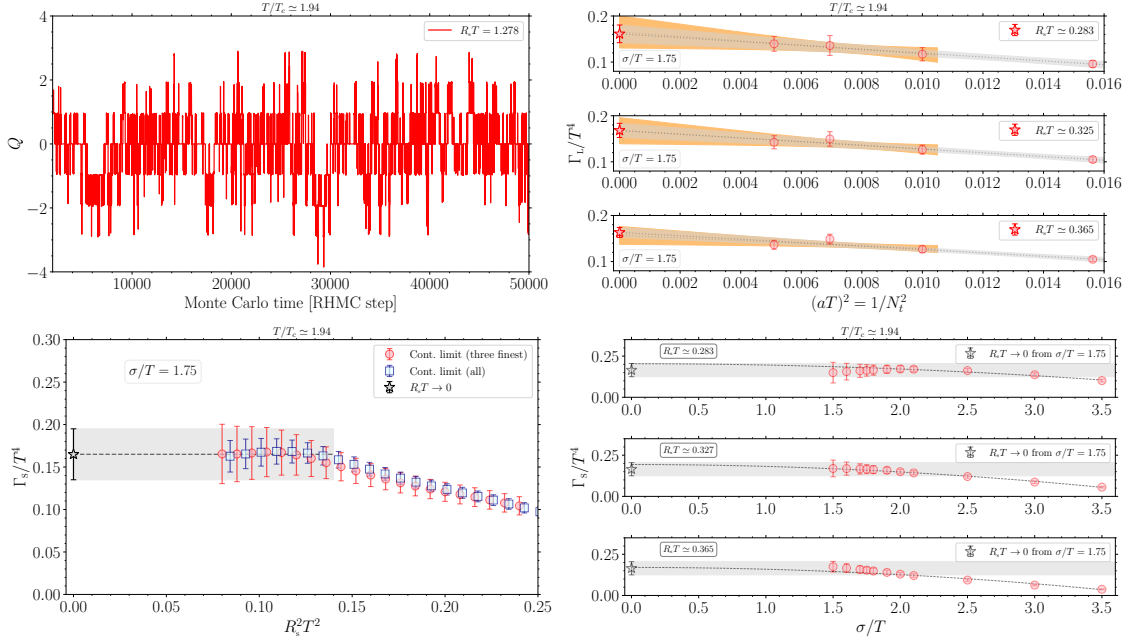


**Figure 5:** Example of the calculation of the sphaleron rate for  $T = 300 \text{ MeV} \approx 1.94T_c$ . Top left panel: Monte Carlo evolution of the cooled clover lattice topological charge for the finest lattice spacing explored at this temperature,  $aT = 1/14$ . Top right panel: continuum limit of  $\Gamma_S/T^4$  at fixed  $\sigma/T = 1.75$  and  $R_S T$  for the three smallest smoothing radii explored. Bottom left panel: smoothing-radius dependence of the continuum results for  $\Gamma_S/T^4$  (fixed  $\sigma/T = 1.75$ ). Bottom right panel: smearing-width dependence of the continuum results for  $\Gamma_S/T^4$  at fixed  $R_S/T$  for the three smallest smoothing radii explored. Figures from Ref. [2].

independent of the smoothing radius in the continuum limit. Finally, the bottom right panel shows the  $\sigma/T$ -dependence of the continuum determinations of  $\Gamma_S/T^4$  for the 3 smallest values of  $R_S T$  explored (thus all lying in the plateau previously identified). The general theoretical expectation for an even smearing kernel  $\Delta(\omega) = \Delta(-\omega)$  like ours is that [68]:

$$\Gamma_S(\sigma) = \Gamma_S(0) [1 + O(\sigma^2)]. \quad (25)$$

The results shown in Fig. 5 are in agreement with this prediction. Indeed, below  $\sigma/T \approx 2$  one observes that the sphaleron rate becomes rather insensitive to the smearing width, signaling that the smeared spectral density computed from HLT faithfully represents the physical one in this regime, and that  $O(\sigma^2)$  corrections become smaller than our statistical uncertainties. This result is further corroborated by the fact that explicit  $\sigma/T \rightarrow 0$  extrapolations according to Eq. (25), involving also results obtained for  $\sigma/T > 2$ , all turn out to be compatible with the value at the plateau observed in the bottom left panel of Fig. 5 for  $\sigma/T = 1.75$ . Therefore, that value is taken to be our final result for  $\Gamma_S/T^4$ .

### 3.2 The temperature-dependence of the QCD sphaleron rate

The temperature-dependence of the QCD sphaleron rate is shown in Fig. 6, where we compare it with pure-gauge results of [48], and with the semiclassical computation of [47]. The comparison is performed in terms of  $T/T_c$ , where for the pure-gauge theory the value of the critical deconfinement

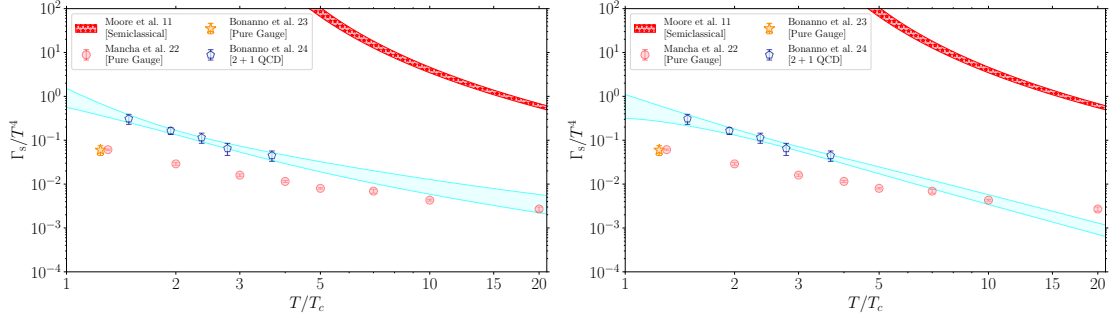


**Figure 6:** Temperature dependence of the sphaleron rate in 2+1 QCD [2] compared to the temperature dependence in the pure gauge theory [48], and to the one expected from semiclassics [47]. The blue bands represent, respectively, the best fit of the full QCD data to the ansatz in Eq. (27) (left panel), and to the ansatz in Eq. (28) (right panel). The starred point stands for the result obtained in [1] in the pure gauge theory, using the same method employed in full QCD. It is a non-trivial cross-check, as it agrees with the result of [48], obtained without resorting to any inverse problem resolution, at a close-by temperature. Figures from Ref. [2].

temperature  $T_c \simeq 287$  MeV was used. Interestingly, unlike what happens with the topological susceptibility, the sphaleron rate is not suppressed by the presence of light dynamical quarks. This is likely due to the fact that  $\Gamma_s$  receives dominant contribution from the large- $\tau$  tail of  $G_E(\tau)$ , which is not expected to be suppressed by light dynamical fermions. Our new method [1] was cross-checked in the pure gauge theory against the result of [48] for a near-by temperature, finding perfect agreement. This is highly non-trivial, given that the results of [48] were obtained with a completely different method, not relying on the inverse problem resolution.

In Ref. [2], we tried two different Ansätze to fit the  $T$ -dependence of  $\Gamma_s/T^4$ . One is rooted on the semiclassical result of [47]:

$$\Gamma_s \propto \alpha_s^5(T), \quad (26)$$

and in the 1-loop running of  $\alpha_s(\mu) \propto 1/\log(\mu/\Lambda_{\text{QCD}})$ . In particular, we employed the following fit function:

$$\frac{\Gamma_s}{T^4} = \left( \frac{A}{\log x + B} \right)^C, \quad x = T/T_c. \quad (27)$$

Fixing  $C = 5$  (as per the semiclassical prediction) gives an excellent description of the data, shown in the left panel of Fig. 6 as a shaded band. However, leaving  $C$  as a free parameter gives  $C \simeq 5.6$  with a 100% uncertainty. Thus, we cannot claim we have determined the exponent in the functional form in Eq. (27), as the explored temperature range is too narrow. We also tried a power-law functional form of the type:

$$\frac{\Gamma_s}{T^4} = A \frac{1}{x^C}, \quad x = T/T_c. \quad (28)$$

Also in this case one finds an excellent description of the data, and an exponent  $C \simeq 2.19(38)$ . The result is shown in the right panel of Fig. 6 as a shaded band. Clarifying the actual temperature dependence of the sphaleron rate requires calculations at larger temperatures of the order of 1 GeV, i.e.,  $T/T_c \sim \mathcal{O}(10)$ .

#### 4. Conclusions and the road ahead

The results of Ref. [2] have clearly demonstrated that, using the novel method of [1], one can reliably determine the non-perturbative QCD sphaleron rate from the lattice with an excellent control over several sources of systematic errors (finite lattice spacing, finite smearing width, finite smoothing radius). Now that this new avenue of research has been opened, it would be interesting to further push the first investigation of Ref. [2] towards the regimes that are interesting for phenomenological applications. Two examples would be to extend the temperature range towards the GeV scale, and to explore the momentum dependence of the topological rate in Eq. (5), both of which are necessary inputs for axion phenomenology.

To complete these tasks one has to face a serious computational challenge. Indeed, reaching temperatures of the order of 1 GeV on lattices which have at least  $N_t \sim 12 - 16$  temporal sites (a necessary requirement to avoid significant lattice artifacts), requires lattice spacings of the order of  $a \sim 0.02 - 0.01$  fm. It is well known that pushing Lattice QCD simulations towards this regime is very hard due to the infamous topological freezing computational problem [6, 89–91]. In a few words, when approaching the continuum limit, standard Monte Carlo updating algorithms severely lose ergodicity, especially when focusing on the sampling of the topological charge. In practice, this manifests in a dramatic growth of the number of updating steps necessary to generate two decorrelated samples of the topological charge as  $a \rightarrow 0$ . Apart from this major issue, one should also take into account that the 2 + 1 setup employed in Ref. [2] is not adequate to reach  $T \sim 1$  GeV since, at that scale, the dynamical charm quark contribution becomes non-negligible, being  $m_c/T \sim O(1)$ . The latter point, in particular, implies that one ought to push 2 + 1 + 1 scale setting towards lattice spacings as fine as  $a \sim 0.01$  fm to reliably simulate QCD around a 1 GeV temperature, something that is again computationally highly non-trivial (especially because of topological freezing).

In recent years, there were significant efforts in devising new strategies to defeat topological freezing, targeted towards performing efficient simulations on very fine lattices, see, e.g., Refs. [3, 92–102]. Among these proposals, me and my collaborators have extensively employed a new algorithmic solution that allows to efficiently avoid topological freezing down to extremely fine lattice spacings: *Parallel Tempering on Boundary Conditions* (PTBC) [3, 14, 35, 103–108]. In particular, in the recent study [3], we first implemented it in 2+1 QCD at the physical point obtaining significant improvements with respect to the standard RHMC. This is clearly illustrated in Fig. 7, which reports determinations of the QCD topological susceptibility at zero and high temperature via PTBC and standard RHMC.

The left panel of Fig. 7 shows the topological susceptibility in the  $T = 0$  case, where lattice results can be compared with the prediction obtained from next-to-leading order (NLO) Chiral Perturbation Theory ( $\chi$ PT) [109] (see also [110]). As it can be seen, at the fairly fine lattice spacing  $a \simeq 0.056$  fm the lattice result for  $\chi$  is still off by about a factor of 2 compared to the NLO  $\chi$ PT prediction. This is due to the presence of large lattice artifacts affecting  $\chi$  in the presence of light dynamical quarks [15]. Going below this threshold is hard with standard methods due to topological freezing, and this is reflected in the large errors affecting the susceptibility determined for finer lattice spacings with standard methods. The PTBC algorithm instead, significantly reduces autocorrelation times of the topological charge, allowing a reliable determination of  $\chi$  in this

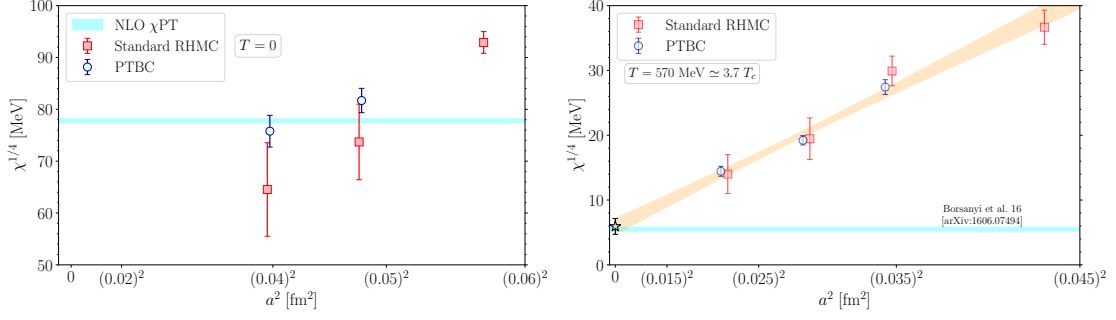


**Figure 7:** Improvement obtained adopting the PTBC algorithm in the determination of the topological susceptibility in  $2 + 1$  QCD at the physical point with respect to the standard RHMC algorithm. Left panel: zero temperature case. Right panel: results for  $T = 570 \text{ MeV} \approx 3.7 T_c$ . Figures from Ref. [3].

regime. As it can be seen, PTBC results obtained down to  $a \approx 0.04 \text{ fm}$  are much more accurate, and in nice agreement with the NLO  $\chi$ PT result. The right panel of Fig. 7 shows instead the finite-temperature case, where the obtained improvement is even more impressive. In that case, we pushed our investigation down to  $a \approx 0.02 \text{ fm}$ , and could achieve a huge improvement in the continuum determination of  $\chi$ . Our final result is found to be in agreement with the result of [17], obtained with an indirect method, based on a low-lying Dirac eigenvalue reweighting of the gauge configurations to reduce lattice artifacts by hand.

In conclusion, thanks to the improvements yielded by the PTBC algorithm, I anticipate major progress in the next future about the study of QCD topology from the lattice. These will concern both the study of the topological susceptibility and of the sphaleron rate in the regimes relevant for physical applications, most importantly axion cosmology and collider physics inputs.

## Acknowledgments

I would like to thank Massimo D’Elia and Margarita García Pérez for reading this article. I acknowledge support from the Spanish Research Agency (Agencia Estatal de Investigación) through the grant IFT Centro de Excelencia Severo Ochoa CEX2020-001007-S and, partially, by the grant PID2021-127526NB-I00, both funded by MCIN/AEI/10.13039/501100011033. Numerical simulations of Refs. [1–3] have been performed on the Marconi, Marconi100, and Leonardo machines at Cineca, based on the agreement between INFN and Cineca, under projects INF22\_npqcd, INF23\_npqcd, and INF24\_npqcd.

## References

- [1] C. Bonanno, F. D’Angelo, M. D’Elia, L. Maio and M. Naviglio, *Sphaleron rate from a modified Backus-Gilbert inversion method*, *Phys. Rev. D* **108** (2023) 074515 [2305.17120].
- [2] C. Bonanno, F. D’Angelo, M. D’Elia, L. Maio and M. Naviglio, *Sphaleron Rate of  $N_f = 2 + 1$  QCD*, *Phys. Rev. Lett.* **132** (2024) 051903 [2308.01287].
- [3] C. Bonanno, G. Clemente, M. D’Elia, L. Maio and L. Parente, *Full QCD with milder topological freezing*, *JHEP* **08** (2024) 236 [2404.14151].

- [4] E. Witten, *Current Algebra Theorems for the  $U(1)$  Goldstone Boson*, *Nucl. Phys. B* **156** (1979) 269.
- [5] G. Veneziano,  *$U(1)$  Without Instantons*, *Nucl. Phys. B* **159** (1979) 213.
- [6] L. Del Debbio, H. Panagopoulos and E. Vicari,  *$\theta$  dependence of  $SU(N)$  gauge theories*, *JHEP* **08** (2002) 044 [[hep-th/0204125](#)].
- [7] L. Del Debbio, L. Giusti and C. Pica, *Topological susceptibility in the  $SU(3)$  gauge theory*, *Phys. Rev. Lett.* **94** (2005) 032003 [[hep-th/0407052](#)].
- [8] C. Bonati, M. D’Elia and A. Scapellato,  *$\theta$  dependence in  $SU(3)$  Yang-Mills theory from analytic continuation*, *Phys. Rev. D* **93** (2016) 025028 [[1512.01544](#)].
- [9] M. Cè, C. Consonni, G. P. Engel and L. Giusti, *Non-Gaussianities in the topological charge distribution of the  $SU(3)$  Yang–Mills theory*, *Phys. Rev. D* **92** (2015) 074502 [[1506.06052](#)].
- [10] C. Bonati, M. D’Elia, P. Rossi and E. Vicari,  *$\theta$  dependence of 4D  $SU(N)$  gauge theories in the large- $N$  limit*, *Phys. Rev. D* **94** (2016) 085017 [[1607.06360](#)].
- [11] M. Cè, M. Garcia Vera, L. Giusti and S. Schaefer, *The topological susceptibility in the large- $N$  limit of  $SU(N)$  Yang-Mills theory*, *Phys. Lett. B* **762** (2016) 232 [[1607.05939](#)].
- [12] A. Athenodorou and M. Teper, *The glueball spectrum of  $SU(3)$  gauge theory in  $3 + 1$  dimensions*, *JHEP* **11** (2020) 172 [[2007.06422](#)].
- [13] A. Athenodorou and M. Teper,  *$SU(N)$  gauge theories in  $3+1$  dimensions: glueball spectrum, string tensions and topology*, *JHEP* **12** (2021) 082 [[2106.00364](#)].
- [14] C. Bonanno, *The large- $N$  limit of the topological susceptibility of  $SU(N)$  Yang-Mills theories via Parallel Tempering on Boundary Conditions*, *JHEP* **01** (2026) 039 [[2510.08006](#)].
- [15] C. Bonati, M. D’Elia, M. Mariti, G. Martinelli, M. Mesiti, F. Negro et al., *Axion phenomenology and  $\theta$ -dependence from  $N_f = 2 + 1$  lattice QCD*, *JHEP* **03** (2016) 155 [[1512.06746](#)].
- [16] P. Petreczky, H.-P. Schadler and S. Sharma, *The topological susceptibility in finite temperature QCD and axion cosmology*, *Phys. Lett. B* **762** (2016) 498 [[1606.03145](#)].
- [17] S. Borsanyi et al., *Calculation of the axion mass based on high-temperature lattice quantum chromodynamics*, *Nature* **539** (2016) 69 [[1606.07494](#)].
- [18] A. Trunin, F. Burger, E.-M. Ilgenfritz, M. P. Lombardo and M. Müller-Preussker, *Topological susceptibility from  $N_f = 2 + 1 + 1$  lattice QCD at nonzero temperature*, *J. Phys. Conf. Ser.* **668** (2016) 012123 [[1510.02265](#)].
- [19] F. Burger, E.-M. Ilgenfritz, M. P. Lombardo, M. Müller-Preussker and A. Trunin, *Topology (and axion’s properties) from lattice QCD with a dynamical charm*, *Nucl. Phys. A* **967** (2017) 880 [[1705.01847](#)].

- [20] C. Bonati, M. D’Elia, G. Martinelli, F. Negro, F. Sanfilippo and A. Todaro, *Topology in full QCD at high temperature: a multicanonical approach*, *JHEP* **11** (2018) 170 [1807.07954].
- [21] F. Burger, E.-M. Ilgenfritz, M. P. Lombardo and A. Trunin, *Chiral observables and topology in hot QCD with two families of quarks*, *Phys. Rev. D* **98** (2018) 094501 [1805.06001].
- [22] M. P. Lombardo and A. Trunin, *Topology and axions in QCD*, *Int. J. Mod. Phys. A* **35** (2020) 2030010 [2005.06547].
- [23] A. Athenodorou, C. Bonanno, C. Bonati, G. Clemente, F. D’Angelo, M. D’Elia et al., *Topological susceptibility of  $N_f = 2 + 1$  QCD from staggered fermions spectral projectors at high temperatures*, *JHEP* **10** (2022) 197 [2208.08921].
- [24] A. Y. Kotov, M. P. Lombardo and A. Trunin, *Topological observables and  $\theta$  dependence in high temperature QCD from lattice simulations*, *JHEP* **09** (2025) 045 [2502.15407].
- [25] A. Shindler, T. Luu and J. de Vries, *Nucleon electric dipole moment with the gradient flow: The  $\theta$ -term contribution*, *Phys. Rev. D* **92** (2015) 094518 [1507.02343].
- [26] F. K. Guo, R. Horsley, U. G. Meissner, Y. Nakamura, H. Perlt, P. E. L. Rakow et al., *The electric dipole moment of the neutron from 2+1 flavor lattice QCD*, *Phys. Rev. Lett.* **115** (2015) 062001 [1502.02295].
- [27] J. Dragos, T. Luu, A. Shindler, J. de Vries and A. Yousif, *Confirming the Existence of the strong CP Problem in Lattice QCD with the Gradient Flow*, *Phys. Rev. C* **103** (2021) 015202 [1902.03254].
- [28] C. Alexandrou, A. Athenodorou, K. Hadjiyiannakou and A. Todaro, *Neutron electric dipole moment using lattice QCD simulations at the physical point*, *Phys. Rev. D* **103** (2021) 054501 [2011.01084].
- [29] T. Bhattacharya, V. Cirigliano, R. Gupta, E. Mereghetti and B. Yoon, *Contribution of the QCD  $\Theta$ -term to the nucleon electric dipole moment*, *Phys. Rev. D* **103** (2021) 114507 [2101.07230].
- [30]  $\chi$ QCD collaboration, J. Liang, A. Alexandru, T. Draper, K.-F. Liu, B. Wang, G. Wang et al., *Nucleon electric dipole moment from the  $\theta$  term with lattice chiral fermions*, *Phys. Rev. D* **108** (2023) 094512 [2301.04331].
- [31] T. Bhattacharya, V. Cirigliano, R. Gupta, E. Mereghetti, J.-S. Yoo and B. Yoon, *Quark chromoelectric dipole moment operator on the lattice*, *Phys. Rev. D* **108** (2023) 074507 [2304.09929].
- [32] M. D’Elia and F. Negro,  *$\theta$  dependence of the deconfinement temperature in Yang–Mills theories*, *Phys. Rev. Lett.* **109** (2012) 072001 [1205.0538].
- [33] M. D’Elia and F. Negro, *Phase diagram of Yang-Mills theories in the presence of a  $\theta$  term*, *Phys. Rev. D* **88** (2013) 034503 [1306.2919].

- [34] N. Otake and N. Yamada,  $\theta$  dependence of  $T_c$  in 4d  $SU(3)$  Yang-Mills theory with histogram method and the Lee-Yang zeros in the large- $N$  limit, *JHEP* **06** (2022) 044 [2202.05605].
- [35] C. Bonanno, M. D’Elia and L. Verzhicelli, The  $\theta$ -dependence of the  $SU(N)$  critical temperature at large  $N$ , *JHEP* **02** (2024) 156 [2312.12202].
- [36] N. Yamada, M. Yamazaki and R. Kitano,  $\theta$  dependence of  $T_c$  in  $SU(2)$  Yang-Mills theory, *JHEP* **02** (2025) 211 [2411.00375].
- [37] N. H. Christ, Conservation Law Violation at High-Energy by Anomalies, *Phys. Rev. D* **21** (1980) 1591.
- [38] F. R. Klinkhamer and N. S. Manton, A Saddle Point Solution in the Weinberg-Salam Theory, *Phys. Rev. D* **30** (1984) 2212.
- [39] F. R. Klinkhamer and P. Nagel,  $SU(3)$  sphaleron: Numerical solution, *Phys. Rev. D* **96** (2017) 016006 [1704.07756].
- [40] G. ’t Hooft, Computation of the Quantum Effects Due to a Four-Dimensional Pseudoparticle, *Phys. Rev. D* **14** (1976) 3432.
- [41] G. ’t Hooft, Symmetry Breaking Through Bell–Jackiw Anomalies, *Phys. Rev. Lett.* **37** (1976) 8.
- [42] W. Busza, K. Rajagopal and W. van der Schee, Heavy Ion Collisions: The Big Picture, and the Big Questions, *Ann. Rev. Nucl. Part. Sci.* **68** (2018) 339 [1802.04801].
- [43] D. E. Kharzeev, L. D. McLerran and H. J. Warringa, The Effects of topological charge change in heavy ion collisions: ’Event by event  $P$  and  $CP$  violation’, *Nucl. Phys. A* **803** (2008) 227 [0711.0950].
- [44] K. Fukushima, D. E. Kharzeev and H. J. Warringa, The Chiral Magnetic Effect, *Phys. Rev. D* **78** (2008) 074033 [0808.3382].
- [45] K. Fukushima, D. E. Kharzeev and H. J. Warringa, Real-time dynamics of the Chiral Magnetic Effect, *Phys. Rev. Lett.* **104** (2010) 212001 [1002.2495].
- [46] D. E. Kharzeev, The Chiral Magnetic Effect and Anomaly-Induced Transport, *Prog. Part. Nucl. Phys.* **75** (2014) 133 [1312.3348].
- [47] G. D. Moore and M. Tassler, The Sphaleron Rate in  $SU(N)$  Gauge Theory, *JHEP* **02** (2011) 105 [1011.1167].
- [48] M. Barroso Mancha and G. D. Moore, The sphaleron rate from 4D Euclidean lattices, *JHEP* **01** (2023) 155 [2210.05507].
- [49] Y. Feng, S. A. Voloshin and F. Wang, Experimental search for the chiral magnetic effect in relativistic heavy-ion collisions: A perspective, *Phys. Rev. Res.* **7** (2025) 031001 [2502.09742].

- [50] A. Notari, F. Rompineve and G. Villadoro, *Improved Hot Dark Matter Bound on the QCD Axion*, *Phys. Rev. Lett.* **131** (2023) 011004 [2211.03799].
- [51] F. Bianchini, G. G. di Cortona and M. Valli, *QCD axion: Some like it hot*, *Phys. Rev. D* **110** (2024) 123527 [2310.08169].
- [52] C. A. J. O’Hare, *Cosmology of axion dark matter*, *PoS COSMICWISPerS* (2024) 040 [2403.17697].
- [53] K. Bouzoud, J. Ghiglieri, M. Laine and G. S. S. Sakoda, *Energy and momentum dependence of the soft-axion interaction rate*, 2601.08221.
- [54] H. B. Meyer, *Transport Properties of the Quark-Gluon Plasma: A Lattice QCD Perspective*, *Eur. Phys. J. A* **47** (2011) 86 [1104.3708].
- [55] P. Lowdon, *Euclidean thermal correlation functions in local QFT*, *Phys. Rev. D* **106** (2022) 045028 [2201.12180].
- [56] A. Y. Kotov, *Sphaleron Transition Rate in Lattice Gluodynamics*, *JETP Letters* **108** (2018) 352.
- [57] L. Altenkort, A. M. Eller, O. Kaczmarek, L. Mazur, G. D. Moore and H.-T. Shu, *Sphaleron rate from Euclidean lattice correlators: An exploration*, *Phys. Rev. D* **103** (2021) 114513 [2012.08279].
- [58] N. Y. Astrakhantsev, V. V. Braguta and A. Y. Kotov, *Temperature dependence of the bulk viscosity within lattice simulation of SU(3) gluodynamics*, *Phys. Rev. D* **98** (2018) 054515 [1804.02382].
- [59] M. Hansen, A. Lupo and N. Tantalo, *Extraction of spectral densities from lattice correlators*, *Phys. Rev. D* **99** (2019) 094508 [1903.06476].
- [60] D. Boito, M. Golterman, K. Maltman and S. Peris, *Spectral-weight sum rules for the hadronic vacuum polarization*, *Phys. Rev. D* **107** (2023) 034512 [2210.13677].
- [61] A. Rothkopf, *Inverse problems, real-time dynamics and lattice simulations*, *EPJ Web Conf.* **274** (2022) 01004 [2211.10680].
- [62] HotQCD collaboration, L. Altenkort, O. Kaczmarek, R. Larsen, S. Mukherjee, P. Petreczky, H.-T. Shu et al., *Heavy Quark Diffusion from 2+1 Flavor Lattice QCD with 320 MeV Pion Mass*, *Phys. Rev. Lett.* **130** (2023) 231902 [2302.08501].
- [63] M. Bruno, L. Giusti and M. Saccardi, *Spectral densities from Euclidean lattice correlators via the Mellin transform*, *Phys. Rev. D* **111** (2025) 094515 [2407.04141].
- [64] L. Del Debbio, A. Lupo, M. Panero and N. Tantalo, *Bayesian solution to the inverse problem and its relation to Backus-Gilbert methods*, *Eur. Phys. J. C* **85** (2025) 185 [2409.04413].

- [65] G. Backus and F. Gilbert, *The Resolving Power of Gross Earth Data*, *Geophysical Journal International* **16** (1968) 169.
- [66] EXTENDED TWISTED MASS COLLABORATION (ETMC) collaboration, C. Alexandrou et al., *Probing the Energy-Smeared R Ratio Using Lattice QCD*, *Phys. Rev. Lett.* **130** (2023) 241901 [2212.08467].
- [67] L. Del Debbio, A. Lupo, M. Panero and N. Tantalo, *Multi-representation dynamics of SU(4) composite Higgs models: chiral limit and spectral reconstructions*, *Eur. Phys. J. C* **83** (2023) 220 [2211.09581].
- [68] R. Frezzotti, N. Tantalo, G. Gagliardi, F. Sanfilippo, S. Simula and V. Lubicz, *Spectral-function determination of complex electroweak amplitudes with lattice QCD*, *Phys. Rev. D* **108** (2023) 074510 [2306.07228].
- [69] EXTENDED TWISTED MASS collaboration, A. Evangelista, R. Frezzotti, N. Tantalo, G. Gagliardi, F. Sanfilippo, S. Simula et al., *Inclusive hadronic decay rate of the  $\tau$  lepton from lattice QCD*, *Phys. Rev. D* **108** (2023) 074513 [2308.03125].
- [70] EXTENDED TWISTED MASS collaboration, C. Alexandrou et al., *Inclusive Hadronic Decay Rate of the  $\tau$  Lepton from Lattice QCD: The  $\bar{u}s$  Flavor Channel and the Cabibbo Angle*, *Phys. Rev. Lett.* **132** (2024) 261901 [2403.05404].
- [71] E. Bennett et al., *Meson spectroscopy from spectral densities in lattice gauge theories*, *Phys. Rev. D* **110** (2024) 074509 [2405.01388].
- [72] A. De Santis et al., *Inclusive semileptonic decays of the  $D_s$  meson: A first-principles lattice QCD calculation*, *Phys. Rev. D* **112** (2025) 054503 [2504.06063].
- [73] A. De Santis et al., *Inclusive Semileptonic Decays of the  $D_s$  Meson: Lattice QCD Confronts Experiments*, *Phys. Rev. Lett.* **135** (2025) 121901 [2504.06064].
- [74] R. Frezzotti, N. Tantalo, G. Gagliardi, V. Lubicz, G. Martinelli, C. T. Sachrajda et al., *Theoretical framework for lattice QCD computations of  $B \rightarrow K\ell^+\ell^-$  and  $\bar{B}_s \rightarrow \ell^+\ell^-\gamma$  decays rates, including contributions from "Charming Penguins"*, *Phys. Rev. D* **113** (2026) 034509 [2508.03655].
- [75] TELOS collaboration, E. Bennett et al., *Chimera baryons and mesons on the lattice: A spectral density analysis*, *Phys. Rev. D* **112** (2025) 074515 [2506.19804].
- [76] B. Berg, *Dislocations and Topological Background in the Lattice O(3)  $\sigma$  Model*, *Phys. Lett. B* **104** (1981) 475.
- [77] Y. Iwasaki and T. Yoshie, *Instantons and Topological Charge in Lattice Gauge Theory*, *Phys. Lett. B* **131** (1983) 159.
- [78] M. Teper, *Instantons in the Quantized SU(2) Vacuum: A Lattice Monte Carlo Investigation*, *Phys. Lett. B* **162** (1985) 357.

- [79] E.-M. Ilgenfritz, M. Laursen, G. Schierholz, M. Müller-Preussker and H. Schiller, *First Evidence for the Existence of Instantons in the Quantized SU(2) Lattice Vacuum*, *Nucl. Phys. B* **268** (1986) 693.
- [80] M. Campostrini, A. Di Giacomo, H. Panagopoulos and E. Vicari, *Topological Charge, Renormalization and Cooling on the Lattice*, *Nucl. Phys. B* **329** (1990) 683.
- [81] R. Narayanan and H. Neuberger, *Infinite N phase transitions in continuum Wilson loop operators*, *JHEP* **03** (2006) 064 [[hep-th/0601210](#)].
- [82] M. Lüscher, *Trivializing maps, the Wilson flow and the HMC algorithm*, *Commun. Math. Phys.* **293** (2010) 899 [[0907.5491](#)].
- [83] M. Lüscher, *Properties and uses of the Wilson flow in lattice QCD*, *JHEP* **08** (2010) 071 [[1006.4518](#)].
- [84] C. Morningstar and M. J. Peardon, *Analytic smearing of SU(3) link variables in lattice QCD*, *Phys. Rev. D* **69** (2004) 054501 [[hep-lat/0311018](#)].
- [85] C. Bonati and M. D’Elia, *Comparison of the gradient flow with cooling in SU(3) pure gauge theory*, *Phys. Rev. D* **D89** (2014) 105005 [[1401.2441](#)].
- [86] C. Alexandrou, A. Athenodorou, K. Cichy, A. Dromard, E. Garcia-Ramos, K. Jansen et al., *Comparison of topological charge definitions in Lattice QCD*, *Eur. Phys. J. C* **80** (2020) 424 [[1708.00696](#)].
- [87] C. Bonati and M. D’Elia, *Topological critical slowing down: variations on a toy model*, *Phys. Rev. E* **98** (2018) 013308 [[1709.10034](#)].
- [88] P. T. Jahn, G. D. Moore and D. Robaina,  $\chi_{top}(T \gg T_c)$  in pure-gluon QCD through reweighting, *Phys. Rev. D* **98** (2018) 054512 [[1806.01162](#)].
- [89] B. Allés, G. Boyd, M. D’Elia, A. Di Giacomo and E. Vicari, *Hybrid Monte Carlo and topological modes of full QCD*, *Phys. Lett. B* **389** (1996) 107 [[hep-lat/9607049](#)].
- [90] L. Del Debbio, G. M. Manca and E. Vicari, *Critical slowing down of topological modes*, *Phys. Lett. B* **594** (2004) 315 [[hep-lat/0403001](#)].
- [91] ALPHA collaboration, S. Schaefer, R. Sommer and F. Virotta, *Critical slowing down and error analysis in lattice QCD simulations*, *Nucl. Phys. B* **845** (2011) 93 [[1009.5228](#)].
- [92] L. Giusti and M. Lüscher, *Topological susceptibility at  $T > T_c$  from master-field simulations of the SU(3) gauge theory*, *Eur. Phys. J. C* **79** (2019) 207 [[1812.02062](#)].
- [93] L. Funcke, K. Jansen and S. Kühn, *Topological vacuum structure of the Schwinger model with matrix product states*, *Phys. Rev. D* **101** (2020) 054507 [[1908.00551](#)].
- [94] G. Kanwar, M. S. Albergo, D. Boyda, K. Cranmer, D. C. Hackett, S. Racanière et al., *Equivariant flow-based sampling for lattice gauge theory*, *Phys. Rev. Lett.* **125** (2020) 121601 [[2003.06413](#)].

- [95] D. Albande, P. Hernández, A. Ramos and F. Romero-López, *Topological sampling through windings*, *Eur. Phys. J. C* **81** (2021) 873 [2106.14234].
- [96] G. Cossu, D. Lancastera, B. Lucini, R. Pellegrini and A. Rago, *Ergodic sampling of the topological charge using the density of states*, *Eur. Phys. J. C* **81** (2021) 375 [2102.03630].
- [97] S. Borsanyi and D. Sexty, *Topological susceptibility of pure gauge theory using Density of States*, *Phys. Lett. B* **815** (2021) 136148 [2101.03383].
- [98] K. Cranmer, G. Kanwar, S. Racanière, D. J. Rezende and P. E. Shanahan, *Advances in machine-learning-based sampling motivated by lattice quantum chromodynamics*, *Nature Rev. Phys.* **5** (2023) 526 [2309.01156].
- [99] T. Eichhorn, G. Fuwa, C. Hoelbling and L. Varnhorst, *Parallel tempered metadynamics: Overcoming potential barriers without surfing or tunneling*, *Phys. Rev. D* **109** (2024) 114504 [2307.04742].
- [100] D. Howarth and A. J. Peterson, *Topological charge unfreezing with AMReX*, 2312.11599.
- [101] M. Abe, O. Morikawa and H. Suzuki, *Monte Carlo Simulation of the SU(2)/ $\mathbb{Z}_2$  Yang–Mills Theory*, *PTEP* **2025** (2025) 063B03 [2501.00286].
- [102] C. Bonanno, A. Bulgarelli, E. Cellini, A. Nada, D. Panfalone, D. VDACCHINO et al., *Scaling flow-based approaches for topology sampling in SU(3) gauge theory*, 2510.25704.
- [103] M. Hasenbusch, *Fighting topological freezing in the two-dimensional  $CP^{N-1}$  model*, *Phys. Rev. D* **96** (2017) 054504 [1706.04443].
- [104] C. Bonanno, C. Bonati and M. D’Elia, *Large- $N$  SU( $N$ ) Yang–Mills theories with milder topological freezing*, *JHEP* **03** (2021) 111 [2012.14000].
- [105] C. Bonanno, M. D’Elia, B. Lucini and D. VDACCHINO, *Towards glueball masses of large- $N$  SU( $N$ ) pure-gauge theories without topological freezing*, *Phys. Lett. B* **833** (2022) 137281 [2205.06190].
- [106] C. Bonanno, J. L. Dasilva Golán, M. D’Elia, M. García Pérez and A. Giorgieri, *The SU(3) twisted gradient flow strong coupling without topological freezing*, *Eur. Phys. J. C* **84** (2024) 916 [2403.13607].
- [107] C. Bonanno, C. Bonati, M. Papace and D. VDACCHINO, *The  $\theta$ -dependence of the Yang–Mills spectrum from analytic continuation*, *JHEP* **05** (2024) 163 [2402.03096].
- [108] C. Bonanno, J. L. Dasilva Golán, M. García Pérez, M. D’Elia and A. Giorgieri, *Scale setting of SU( $N$ ) Yang–Mills theory, topology and large- $N$  volume independence*, 2511.07355.
- [109] G. Grilli di Cortona, E. Hardy, J. Pardo Vega and G. Villadoro, *The QCD axion, precisely*, *JHEP* **01** (2016) 034 [1511.02867].
- [110] M. Gorghetto and G. Villadoro, *Topological Susceptibility and QCD Axion Mass: QED and NNLO corrections*, *JHEP* **03** (2019) 033 [1812.01008].